5. Zuo, J. M. Quantitative convergent beam electron diffraction. *Mater. Trans. JIM* **39,** 938–946 (1998).
6. O'Keeffe, M. Madelung constants for the C3 and C9 structures. *J. Chem. Phys.* **38,** 3035–3038 (1963).
7. Coppens, P. *X-ray Charge Densities and Chemical Bonding* (Oxford, New York, 1997).
8. Koritsanszky, T. *et al.* Accurate experimental electronic properties of DL-proline monohydrate obtained within 1 day. *Science* **279,** 356–358 (1998).
9. Stewart, R. F. & Spackman, M. in *Structure and Bonding in Crystals* (eds O'Keeffe, M. & Navrotsky, A.) 279–298 (Academic, New York, 1981).
10. Smart, D. J. & Humphreys, C. J. The application of electron diffraction to determining bonding charge densities in crystals. *Int. Phys. Conf. Ser.* **52,** 211–214 (1980).
11. Restori, R. & Schwarzenbach, D. Charge density in cuprite, Cu_2O. *Acta Crystallogr. B* **42,** 201–208 (1986).
12. Kirfel, A. & Eichhorn, K. Accurate structure analysis with synchrotron radiation, the electron density in Al_2O_3 and Cu_2O. *Acta Crystallogr. A* **46,** 271–284 (1990).
13. Stewart, R. F. Electron population analysis with rigid pseudoatoms. *Acta Crystallogr. A* **32,** 565–574 (1976).
14. Rez, D., Rez, P. & Grant, I. Dirac-Fock calculations of X-ray-scattering factors and contributions to the mean inner potential for electron-scattering. *Acta Crystallogr. A* **50,** 481–497 (1994); correction **53,** 522 (1997).
15. Blaha, P., Schwarz, K. & Luitz, J. WIEN97 (Vienna Univ. of Technol., Vienna, 1997).
16. Blaha, P., Schwarz, K., Sorantin, P. & Trickey, S. B. Full-potential, linearized augmented plane-wave programs for crystalline systems. *Comput. Phys. Commun.* **59,** 399–415 (1990).
17. Marksteiner, P., Blaha, P. & Schwarz, K. Electronic structure and binding mechanism of Cu_2O. *Z. Phys. B* **64,** 119–127 (1986).
18. Zuo, J. M., Blaha, P. & Schwarz, K. The theoretical charge density of silicon: experimental test of exchange and correlation potentials. *J. Phys. Condens. Matt.* **9,** 7541–7561 (1997).
19. Ghijsen, J. *et al.* Electronic structure of Cu_2O and CuO. *Phys. Rev. B* **38,** 11322–11330 (1988).

Acknowledgements

We thank A. Avilov for discussions, and D. Schwarzenbach for providing the X-ray data. This work was supported by the NSF.

Correspondence and requests for materials should be addressed to J.M.Z. (e-mail: Zuo@asu.edu).

Discerning vibronic molecular dynamics using time-resolved photoelectron spectroscopy

Valérie Blanchet, Marek Z. Zgierski, Tamar Seideman & Albert Stolow

Steacie Institute for Molecular Sciences, National Research Council of Canada, Ottawa, Ontario, Canada K1A 0R6

Dynamic processes at the molecular level occur on ultrafast time scales and are often associated with structural as well as electronic changes. These can in principle be studied by time-resolved scattering[1–3] and spectroscopic methods, respectively. In polyatomic molecules, however, excitation results in the rapid mixing of vibrational and electronic motions, which induces both charge redistribution and energy flow in the molecule[4,5]. This 'vibronic' or 'non-adiabatic' coupling is a key step in photochemical[6] and photobiological processes[7] and underlies many of the concepts of molecular electronics[8], but it obscures the notion of distinct and readily observable vibrational and electronic states. Here we report time-resolved photoelectron spectroscopy measurements that distinguish vibrational dynamics from the coupled electronic population dynamics, associated with the photo-induced internal conversion, in a linear unsaturated hydrocarbon chain. The vibrational resolution of our photoelectron spectra allows for a direct observation of the underlying nuclear dynamics, demonstrating that it is possible to obtain detailed insights into ultrafast non-adiabatic processes.

The Born-Oppenheimer approximation (BOA), an adiabatic separation of electronic from nuclear motions, has the pivotal role in defining the potential energy surface and thus permits a mechanistic picture of molecular dynamics. The breakdown of the BOA is due to the motions of the atoms near the intersections of potential surfaces belonging to different electronic states. This mixing of vibrational and electronic motions in excited molecules can in principle be inferred from both frequency-resolved and time-resolved optical spectroscopies. Time-resolved experiments may be generally understood as preparing an excited state with a pump pulse and then, as a function of time, projecting it with a probe pulse onto a final state which acts as a template[9–17]. Ideally, the final state should be well characterized. Photoionization detection has several conceptual and practical advantages[10]. The ion state may be well characterized by independent methods such as high resolution photoelectron spectroscopy and *ab initio* computation. Photoelectron detection has the additional advantage that the signal may be dispersed with respect to kinetic energy and angular distribution. Photoelectron spectroscopy has, compared with optical spectroscopies, fairly relaxed selection rules: any molecular state can be ionized (no 'dark' states). A simplified but very useful picture is that emission of an independent outer electron can occur without the simultaneous electronic reorganization of the ion core (Koopmans' approximation). Partial photoionization probabilities can differ drastically with respect to the molecular orbital nature of the neutral electronic state. If a given electronic configuration correlates—upon removal of the outermost electron—to the electronic configuration of the ground electronic state of the cation, then the corresponding photoionization probability is much higher than if it does not.

Time-resolved photoelectron spectroscopy (TRPES) has been proposed as a technique for the study of ultrafast non-adiabatic processes[10–14] and spin–orbit coupling[15] in isolated polyatomic molecules. The TRPES method has been shown to provide details

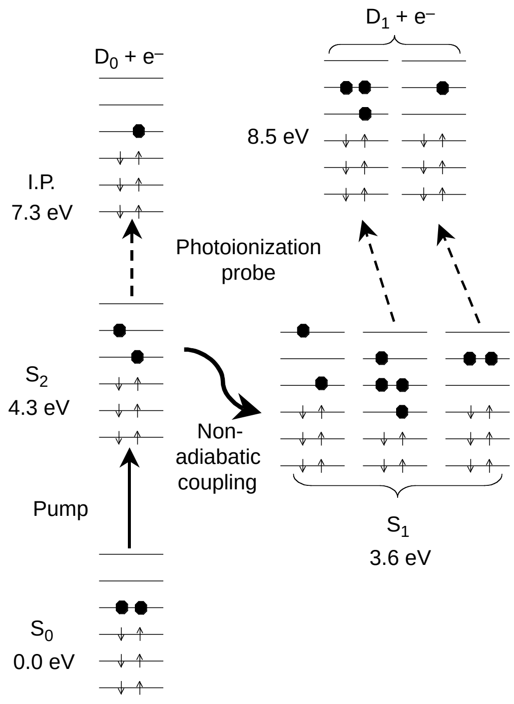

Figure 1 Molecular orbital configurations and photoionization correlations in all-*trans* 2,4,6,8 decatetraene, DT. The optically coupled S_2 (excitation at 4.3 eV shown by straight solid arrow) state is a singly excited configuration, whereas the lower-lying optically forbidden S_1 (3.6 eV) state is composed of both singly and doubly excited configurations. The curved solid arrow indicates non-adiabatic coupling in the excited state. On removal of the highest-lying electron, S_2 correlates with the D_0 cation ground-state configuration with an ionization potential (I.P.) of 7.3 eV, whereas S_1 correlates predominantly with the D_1 cation excited-state configurations at 8.5 eV. it is therefore expected, assuming a single active electron, that the photoionization electronic channel should switch from $D_0 + e^-$ to $D_1 + e^-$ during the $S_2 \rightarrow S_1$ internal conversion. The dashed arrows indicate the most probable ionization channels.

of vibrational dynamics in simple molecules on single potential surfaces[10,16,17]. In polyatomic molecules, non-adiabatic coupling leads to an evolving electronic state symmetry and therefore a changing correlation upon ionization. A switching of the photoelectron band is expected, providing a record of the electronic population dynamics. The detailed vibrational structure of each band simultaneously reveals the nuclear dynamics in each of the coupled electronic states.

We demonstrate our method by studying ultrafast internal conversion in a linear polyene: all-*trans* 2,4,6,8 decatetraene (DT, $C_{10}H_{14}$). Linear polyenes are hydrocarbon chains that have long been an area of fundamental and applied research[18]. Their non-adiabatic dynamics leads to the fundamental process of *cis–trans* photoisomerization. Polyenes form the light-harvesting antennae in vision (rhodopsin) and light-driven transmembrane proton pumps (bacteriorhodopsin). The investigation of polyene photophysics is central to our understanding of electron delocalization and electron correlation in molecules. They have also been used to test quantum chemical theory, as their lowest excited state contains doubly excited configurations[19]. DT provides a classic example of internal conversion in a polyene[20], making it a good candidate for testing our method.

The molecular orbitals that are important in the internal conversion of DT (ionization potential 7.3 eV) can be seen in Fig. 1. These calculated excited electronic states of the molecule and radical cation were obtained with the QCFF/PI + CISD (quantum consistent force field/π-electrons + configuration interaction singles and doubles) method[21,22]. The $S_0(1^1A_g)$ electronic ground state is a single configuration. The first optically allowed transition, at 4.3 eV, is $S_2(1^1B_u) \leftarrow S_0$. The S_2 state is a singly excited configuration. The lowest excited state, however, is the dipole forbidden $S_1(2^1A_g)$ state[23] which arises from configuration interaction between singly and doubly excited A_g configurations, as shown in Fig. 1. Non-adiabatic coupling, leading to ultrafast internal conversion from S_2 to S_1, is promoted by vibrational motions of B_u symmetry. The ionization energies of the continua discussed here are low enough to ensure that the electrons are independent[24] and that Koopmans' approximation applies. The most probable electronic configurations of the cation expected on removal of the highest-lying electron from the neutral excited state are indicated in Fig. 1 by the dashed arrows. It can be seen that the S_2 excited state correlates with the $D_0(1^2B_g)$ ground electronic state of the cation. The S_1 state, by contrast, correlates predominantly with the $D_1(1^2A_u)$ first excited ionic state. We can expect, therefore, a change in the ion state correlation to occur during internal conversion.

Our study of the S_2 to S_1 internal conversion in DT used the femtosecond pump–probe TRPES method described previously[10,11]. In Fig. 2a we show the energy level scheme relevant to this experiment. A femtosecond pump pulse at 287 nm prepared the excited S_2 state at its electronic origin. The system then evolves into a vibrationally hot (0.7 eV) S_1 electronic state via internal conversion. The evolving electronic symmetry is observed by projecting the wavepacket onto several cation electronic states using an ultraviolet probe photon of sufficient energy (here, 235 nm). As the non-adiabatic dynamics proceeds, the changing electronic character alters the photoionization electronic channel, leading to a band switching in the time-resolved photoelectron spectrum.

The experimental photoelectron kinetic energy spectra (Fig. 2b) are characterized by a rapid shift of electrons from an energetic band ($\epsilon_1 = 2.5$ eV) to a broad, structured low-energy band (ϵ_2). This shift is the direct signature of the changing electronic symmetry induced by non-adiabatic coupling. The ϵ_1 band is due to ionization of the S_2 into the D_0 ion state. The ϵ_2 band arises from photoionization of the S_1 state that correlates with the D_1 ion state: its appearance is due to population of the S_1 state by internal conversion. Integration of the photoelectron bands directly reveals the S_2 to S_1 internal conversion timescale of 386 ± 65 fs. A previous estimate[25] based on linewidth measurements was around 0.25 ps.

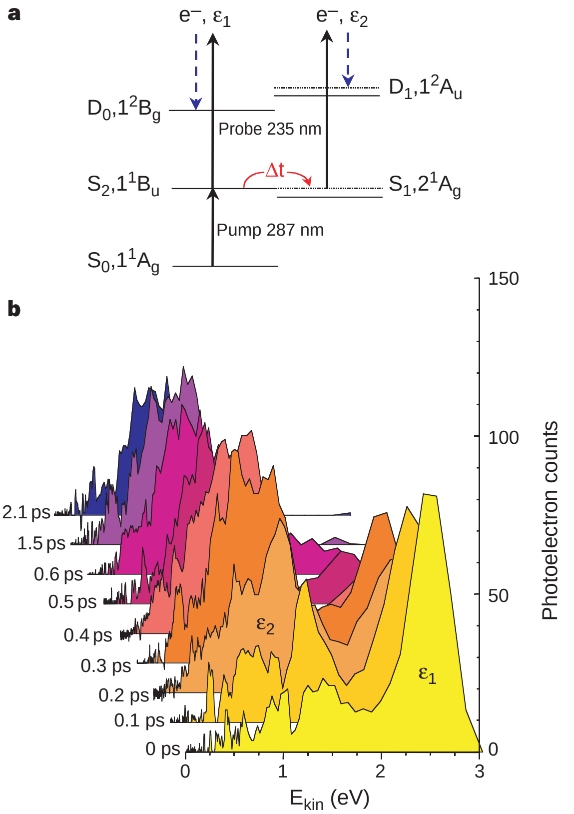

Figure 2 Time-resolved vibrational and electronic dynamics during internal conversion in DT. **a**, Level scheme in DT for one-photon probe ionization. The pump laser prepares the optically bright state S_2. Due to ultrafast internal conversion, this state converts to the lower-lying state S_1 with 0.7 eV of vibrational energy. The expected ionization propensity rules, according to Fig. 1, are shown: $S_2 \rightarrow D_0 + e^-\ (\epsilon_1)$ and $S_1 \rightarrow D_1 + e^-\ (\epsilon_2)$. The dashed lines indicate electron emission. **b**, Femtosecond time-resolved photoelectron kinetic energy (E_{kin}) spectra of DT pumped at 287 nm and probed at 235 nm. There is a rapid shift (~400 fs) in the distribution: from (ϵ_1), an energetic peak at 2.5 eV due to photoionization of S_2 into the D_0 cation ground electronic state; to (ϵ_2), a broad, structured band at lower energies due to photoionization of vibrationally hot S_1 into the D_1 cation first excited electronic state. The structure in the low-energy band reflects the vibrational dynamics in S_1. The time delay between the pump (excitation) and the probe (ionization) laser pulses is indicated by Δt.

We note that the results in Fig. 2 contain much more information than the overall (integrated) internal conversion time. It can be seen that there is vibrational structure in the photoelectron spectra. This structure yields information about the state-to-state vibrational dynamics which promotes and tunes the electronic population transfer, and the ensuing intramolecular vibrational energy redistribution in the 'hot' molecule which occurs on the S_1 potential surface (subjects of our current theoretical investigations).

We have confirmed the above results by comparing them with another scheme using both one- and two-photon ionization. In this case, the first probe photon is above the ionization potential but below D_1 (Fig. 3a). As above, the S_2 state (again prepared at 287 nm) ionizes into D_0, here producing the slow, sharp electron band seen at $\epsilon_1 = 0.4$ eV in Fig. 3b. This band is the same as the $\epsilon_1 = 2.5$ eV band from Fig. 2, but is shifted to lower energy due to the lower-energy probe photon. The band decays rapidly with a time constant of 377 ± 47 fs, providing an independent determination of the $S_2 \rightarrow S_1$ conversion time in agreement with that of Fig. 2. The D_1 ion state is no longer energetically accessible from S_1 via a single photon. At 352 nm, however, our probe laser intensity was sufficient to allow absorption of a second photon. Two-photon ionization accesses different ion electronic states due to the symmetry of the two-photon electric dipole operator, as indicated in Fig. 3a, producing energetic electrons. The S_1 correlations upon two-photon probe ionization can now also include D_0 and D_2 (a higher-lying ion state), producing the broad, energetic ϵ_2 electron bands in Fig. 3b. The switching (at invariant laser intensity) from one-photon to a two-photon favoured ionization again indicates the selectivity of the photoionization process for given electronic state symmetries.

Many photoinduced polyatomic unimolecular reactions are based on vibrationally 'hot' molecules formed via ultrafast internal conversion[26]. A fundamental question in unimolecular reaction rate theory is that of the assumption of statistical energy redistribution due to intramolecular vibrational energy redistribution being very fast compared with reaction[27]. Many models and interpretations are based upon the supposition of fast, complete intramolecular vibrational energy redistribution. Increasingly, however, this assumption has come into question[28]. We believe that our method could present new views of the extent and timescale for the onset of statistical behaviour in an isolated, energized molecule.

Finally, we note possible extensions of the technique we report here. If, for symmetry reasons, the coupled neutral electronic configurations correlate to the same ion electronic configuration, then the electronic–nuclear mixing cannot be clearly discerned by photoelectron kinetic-energy analysis alone. In such cases, the photoelectron angular (that is, partial wave) distributions[29,30], which reflect electron angular-momentum correlations on ionization, should in general still change during a non-adiabatic process. The molecular ionization continuum could provide an interesting template for the study of time-resolved molecular dynamics: ionic vibrational and rotational structure are sensitive to nuclear dynamics, while the ion electronic and the electron partial wave structure are sensitive to electronic population dynamics. We hope that these experimental methods, when combined with dynamical calculations, will provide new insights into the non-adiabatic processes that underpin our understanding of photochemistry, material photosciences and molecular electronics. ☐

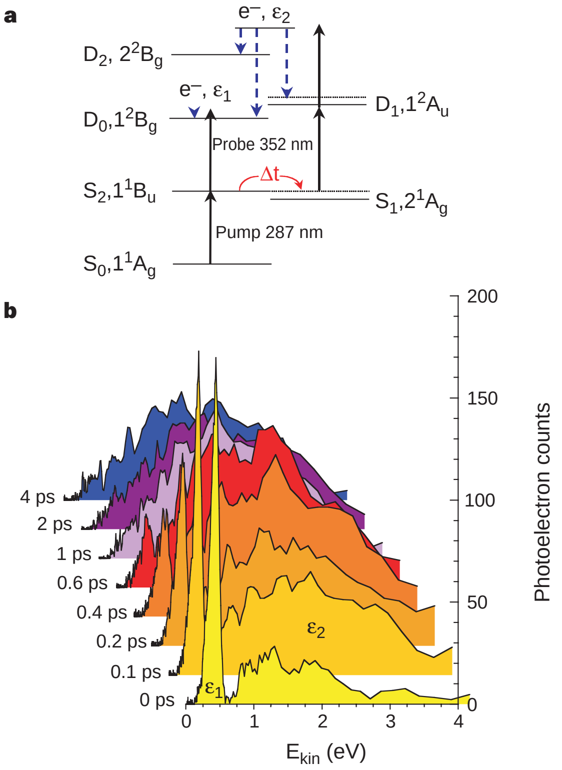

Figure 3 Time-resolved vibrational and electronic dynamics in DT using two-photon ionization. **a**, Level scheme in DT for one- and two-photon probe ionization. The pump laser is identical to that in Fig. 2 and prepares the same S_2 state wavepacket. The expected ionization propensity rules are: $S_2 \longrightarrow D_0 + e^-(\epsilon_1)$ for one-photon ionization (as in Fig. 2) and $S_1 \longrightarrow \longrightarrow D_0, D_1, D_2 + e^-(\epsilon_2)$ for two-photon ionization. The dashed lines indicate electron emission. **b**, Femtosecond time-resolved photoelectron kinetic energy spectra of DT pumped at 287 nm and probed at 352 nm, using both one- and 2-photon probes. At 352 nm, the D_1 ion state is not energetically accessible from the S_1 state via a single photon transition. Confirming the results of Fig. 2, there is a rapid shift (~400 fs) in the distribution: from (ϵ_1) a peak at 0.4 eV due to one-photon ionization of S_2 into the D_0 cation ground electronic state; to (ϵ_2) a broad, structured band at higher energies (1–3.5 eV) due to two-photon ionization of the vibrationally hot S_1 state into the D_0 cation ground and excited electronic states. The photoionization channel switches from a one-photon to a two-photon process during the internal conversion, indicating again that the electronic structure of the ionization continuum is selective of the evolving electronic symmetry in the neutral state.

Received 10 September 1998; accepted 6 July 1999.

1. Rischel, C. *et al.* Femtosecond time-resolved X-ray diffraction from laser-heated organic films. *Nature* **390,** 490–492 (1997).
2. Williamson, J. C., Jianming, C., Hyotcherl, I., Frey, H. & Zewail, A. H. Clocking transient chemical changes by ultrafast electron diffraction. *Nature* **386,** 159–162 (1997).
3. Stepelfeldt, H. Constant, E. & Corkum, P. B. Wavepacket structure and dynamics measured by Coulomb explosion. *Phys. Rev. Lett.* **74,** 3780–3783 (1995).
4. Jortner, J., Rice, S. A. & Hochstrasser, R. M. Radiationless transitions in photochemistry. *Adv. Photochem.* **7,** 149–309 (1969).
5. Stock, G. & Domcke, W. Theory of ultrafast nonadadiabatic excited state processes and their spectroscopic detection in real time. *Adv. Chem. Phys.* **100,** 1–169 (1997).
6. Michl, J. & Bonacic-Koutecky, J. *Electronic Aspects of Organic Photochemistry* (Wiley, New York, 1990).
7. Schoenlein, R. W., Peteanu, L. A., Mathies, R. A. & Shank, C. V. The first step in vision: femtosecond isomerization of rhodopsin. *Science* **254,** 412–415 (1991).
8. Jortner, J. & Ratner, M. A. *Molecular Electronics* (IUPAC, Blackwell, Oxford, 1997).
9. Zewail, A. H. *Femtochemistry: Ultrafast Dynamics of the Chemical Bond* (World Scientific, Singapore, 1994).
10. Fischer, I., Villeneuve, D. M., Vrakking, M. J. J. & Stolow, A. Wavepacket dynamics studied by time-resolved zero-kinetic energy photoelectron spectroscopy. *J. Chem. Phys.* **102,** 5566–5569 (1995).
11. Blanchet, V. & Stolow, A. Non-adiabatic dynamics in polyatomic systems studied by femtosecond time-resolved photoelectron spectroscopy. *J. Chem. Phys.* **108,** 4371–4374 (1998).
12. Seel, M. & Domcke, W. Femtosecond time-resolved ionization spectroscopy of ultrafast internal-conversion dynamics in polyatomic molecules: theory and computational studies. *J. Chem. Phys.* **95,** 7806–7822 (1991).
13. Cyr, D. R. & Hayden, C. C. Femtosecond time-resolved photoionization and photoelectron spectroscopy studies of ultrafast internal conversion in 1,3,5-hexatriene. *J. Chem. Phys.* **104,** 771–774 (1996).
14. Radloff, W. *et al.* Internal conversion in highly excited benzene and benzene dimer: femtosecond time-resolved photoelectron spectroscopy. *Chem. Phys. Lett.* **281,** 20–26 (1997).
15. Kim, B., Schick, C. P. & Weber, P. M. Time-delayed two-colour photoelectron spectra of aniline, 2-aminopyridine and 3-aminopyridine: Snapshots of the nonadiabatic curve crossing. *J. Chem. Phys.* **103,** 6903–6913 (1995).
16. Baumert, T., Thalweiser, R. & Gerber, G. Femtosecond two-photon ionization spectroscopy of the B-state of Na_3 clusters. *Chem. Phys. Lett.* **209,** 29–34 (1993).
17. Assion, A. *et al.* Femtosecond pump-probe photoelectron spectroscopy: Mapping of vibrational wavepacket motion. *Phys. Rev. A* **54,** R4605–R4608 (1996).
18. Hudson, B. S., Kohler, B. E. & Schulten, K. *Excited States* Vol. 6, *Linear Polyene Electronic Structure and Potential Surfaces* (ed. Lim, E. C.) (Academic, New York, 1982).
19. Orlandi, G., Zerbetto, F. & Zgierski, M. Z. Theoretical analysis of spectra of short polyenes. *Chem. Rev.* **91,** 867–891 (1991).
20. Petek, H., Bell, A. J. & Yoshihara, K. & Christensen, R. L. Spectroscopic and dynamical studies of the S_1 and S_2 states of decatetraene in supersonic molecular beams. *J. Chem. Phys.* **95,** 4739–4749 (1991).
21. Warshel, A. & Karplus, M. Calculations of ground and excited state potential surfaces of conjugated molecules. I. Formulation and parametrization. *J. Am. Chem. Soc.* **94,** 5612–5625 (1972).
22. Zerbetto, F., Zgierski, M. Z., Negri, F. & Orlandi, G. Theoretical study of the force fields of the lowest three singlet electronic states of linear polyenes. *J. Chem. Phys.* **89,** 3681–3688 (1988).
23. Andrews, J. R. & Hudson, B. S. Polyene spectroscopy: vibronic evidence for a forbidden transition in deca-2,4,6,8-tetraene. *Chem. Phys. Lett.* **57,** 600–604 (1979).
24. Fronzoni, G., Decleva, P., Lisini, A. & De Alti, G. Ab initio CI investigation of valence photoelectron spectra of conjugated hydrocarbons. *J. Electron. Spectrosc. Relat. Phenom.* **69,** 207–224 (1994).
25. Bouwman, W. G. *et al.* Fluorescence of gaseous tetraenes and pentaenes. *J. Phys. Chem.* **94,** 7429–7434 (1990).
26. Wild, W., Seilmeier, A., Gottfried, N. H. & Kaiser, W. Ultrafast investigations of vibrationally hot molecules after internal conversion in solution. *Chem. Phys. Lett.* **119,** 259–263 (1985).
27. Forst, W. *Theory of Unimolecular Reactions* (Academic, New York, 1973).
28. Remacle, F. & Levine, R. D. Does a dissociating molecule sample the available phase space? *J. Phys. Chem.* **95,** 7124–7127 (1991).
29. Reid, K. L., Duxon, S. P. & Towrie, M. Observation of time- and angle-resolved photoelectron flux from an optically prepared state of a molecule: hyperfine depolarization in NO $A^1\Sigma^+$. *Chem. Phys. Lett.* **228,** 351–356 (1994).
30. Seideman, T. Time-resolved photoelectron angular distributions: a nonperturbative theory. *J. Phys. Chem.* **107,** 7859–7868 (1997).

Acknowledgements

We thank P. Arya and M. Barnes for the synthesis of all-*trans* 2,4,6,8 decatetraene. A.S. thanks W. Domcke, P. B. Corkum and M. Yu. Ivanov for discussions.

Correspondence and requests for materials should be addressed to A.S. (e-mail: albert.stolow@nrc.ca).